# Electronic Supplementary Information

## Detergent-modified catalytic and enzymomimetic activity of silver and palladium nanoparticles biotemplated by *Pyrococcus furiosus* ferritin

*Marie Peskova,[a] Ladislav Ilkovics,[b] David Hynek,[c,d] Simona Dostalova,[c,d] Esther M. Sanchez-Carnerero,[e] Marek Remes,[c,d] Zbynek Heger, [c,d] Vladimir Pekarik,[f,]**

*[a] Central European Institute of Technology (CEITEC), Masaryk University, 625 00 Brno, Czech Republic*
*[b] Institute of Histology and Embryology, Faculty of Medicine, Masaryk University, 625 00 Brno, Czech Republic*
*[c] Department of Chemistry and Biochemistry, Mendel University, 613 00 Brno, Czech Republic, 616 00 Brno, Czech Republic*
*[d] Central European Institute of Technology (CEITEC), Brno University of Technology, 616 00 Brno, Czech Republic*
*[e] RECETOX, Faculty of Science, Masaryk University, Kamenice 5, 625 00, Brno, Czech Republic*
*[f] Institute of Physiology, Faculty of Medicine, Masaryk University, 625 00 Brno, Czech Republic*

** Corresponding author*
*E-mail addresses: pekarikv@mail.muni.cz*

**Contents**:

| Detergent | Abbr. | Final conc. | Detergent type | CMC |
|---|---|---|---|---|
| | | | | |
| Triton X-100 | TX100 | 0.1 % | Non-ionic | 0.2 - 0.9 mM |
| Tween 20 | Tw20 | 0.1 % | Non-ionic | 0.06 mM |
| Sodium caprylate | Capryl | 2.5 mM | Anionic | --- |
| Betaine | Bet | 1 mM | Zwitterionic | --- |
| Pluronic F127 | Plu | 0.1 % | Non-ionic, polymeric | --- |
| Sodium dodecylsulphate | SDS | 1 mM | Anionic | 7 - 10 mM |
| Sodium deoxycholate | DOC | 1 mM | Anionic, bile-acid detergent | 2 - 6 mM |
| Dioctylsulpho succinate | AOT | 1 mM | Anionic | 0.12 - 0.6 mM |
| Cetyltrimethylammonium bromide | CTAB | 1 mM | Cationic | 0.92 mM |
| Nonidet P-40 | NP40 | 1 mM | Non-ionic | 0.06 mM |
| Benzalkonium chloride | BZ | 1 mM | Cationic | --- |
| Tetrabutylammonium bromide | TBAB | 1 mM | Quaternary ammonium salt | --- |

**Table 1**. Used detergents, their abbreviations throughout the text, and final concentrations used in reaction mixtures. TBAB, Capryl, and Bet are low molecular weight detergents and do not form micelles, BZ is mix of several isomers and CMC depends on ration among them. Formation of Plu micelles is very complex and is influenced by the detergent concentration, temperature and ions concentration.

**Synthetic procedures:**

**Synthesis of iodoBODIPY (I.BODIPY)**. 8-[3,5-B is(2 -(2 -(2 -methoxyethoxy)ethoxy)ethoxy)phenyl] -2,6-b is(iodo)-1,3,5,7-tetramethyl-4,4difluoro-4-bora-3a,4a-diaza-*s*-indacene was synthesized according to Park *et al*. [1].

$^1$H NMR (300 MHz, $CDCl_3$): $\delta$ (ppm) 6.63 (t, $J$ = 2.2 Hz, 1H), 6.42 (s, $J$ = 2.2 Hz, 2H), 4.10 (t, $J$ = 4.5 Hz, 4H), 3.84 (t, $J$ = 4.5 Hz, 4H), 3.74-3.71 (m, 4H), 3.69-3.63 (m, 8H), 3.56-3.53 (m, 4H), 3.37 (s, 6H), 2.64 (s, 6H), 1.55 (s, 6H).

**Synthesis of bis-N,N′-propargyloxycarbonyl rhodamine 110 (Proc-R110)**. The synthesis was carried out according to Weiss *et al*.[2]. Briefly, Rhodamine 110 chloride (120 mg, 0.33 mmol) was dissolved in dry DMF (2 ml) under nitrogen atmosphere. Propargyl chloroformate (0.14 ml, 1.31 mmol) and triethylamine (0.23 ml, 1.64 mmol) were added dropwise to the mixture. The reaction mixture was stirred under argon atmosphere at room temperature for 48 h. Solvents were removed under vacuum and the resulting crude re-suspended in 25% isopropanol in DCM (10 ml) and washed with water. The aqueous layer was further washed five times with 25% isopropanol in DCM (5 x 10 ml). The combined organic layers were dried over anhydrous $Na_2SO_4$, the solids were filtered off and the resulting solution was concentrated under vacuum. Crude product was purified via flash chromatography (hexane/ethyl acetate 2:1) and yielded **Proc-R110** as a white solid (18 mg, 11 % yield). $R_f$ = 0.13 (hexane/ethyl acetate 2:1); mass spectrometry (m/z): 495.12 $[M + H]^+$.

**Production and isolation of human FtH and horse Fer8 ferritin.** Plasmid pMK2-Fer8 for production of horse L-chain ferritin Fer8 was gift from Ichiro Yamashita and Naofumi Okamoto [3]. The plasmid for expression of human H-chain ferritin pHsaFtH was kindly

provided by Guangjun Nie [4]. The proteins were produced and purified by the same technique as PfuFt.

**Determination of silver and palladium nanoparticle size from TEM images**. The diameter of individual nanoparticles was individually measured in GIMP2 grogram in pixels. The dimension in nanometers were derived from the pixel size of imbedded scale bar. 200 random nanoparticles were analysed for each type of metal nanoparticles.

**References**


1. Park, J., et al., *Highly selective fluorescence turn-on sensing of gold ions by a nanoparticle generation/C-I bond cleavage sequence.* Analyst, 2012. **137**(19): p. 4411-4.
2. Li, J., et al., *Palladium-triggered deprotection chemistry for protein activation in living cells.* Nat Chem, 2014. **6**(4): p. 352-61.
3. Okuda, M., et al., *Fabrication of nickel and chromium nanoparticles using the protein cage of apoferritin.* Biotechnol Bioeng, 2003. **84**(2): p. 187-94.
4. Sun, C., et al., *Fine-tuned h-ferritin nanocage with multiple gold clusters as near-infrared kidney specific targeting nanoprobe.* Bioconjug Chem, 2015. **26**(2): p. 193-6.


**Figures**:

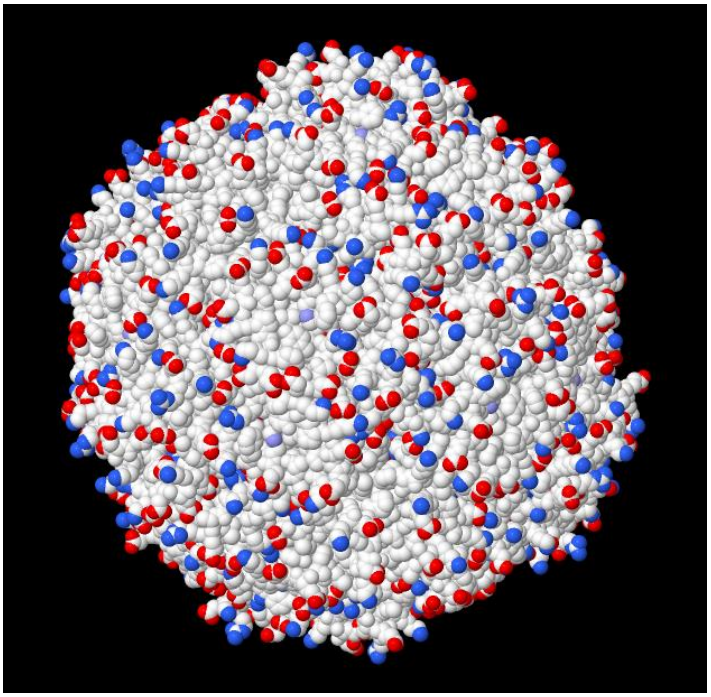

**Figure s1. Surface charge of PfuFt**. The palladium nanoparticles nucleation at the surface of PfuFt is facilitated by coordination of $Pd^{2+}$ ions by surface exposed carboxyl, amino, and

histidyl side chains of aminoacids. Jmol analysis of surface charges of PfuFt (2JD7) showing surface exposed oxygens (red) of aspartic and glutamic acid, nitrogens of arginine and lysine (blue) and histidine (light purple) that are capable of coordination of metal ions.

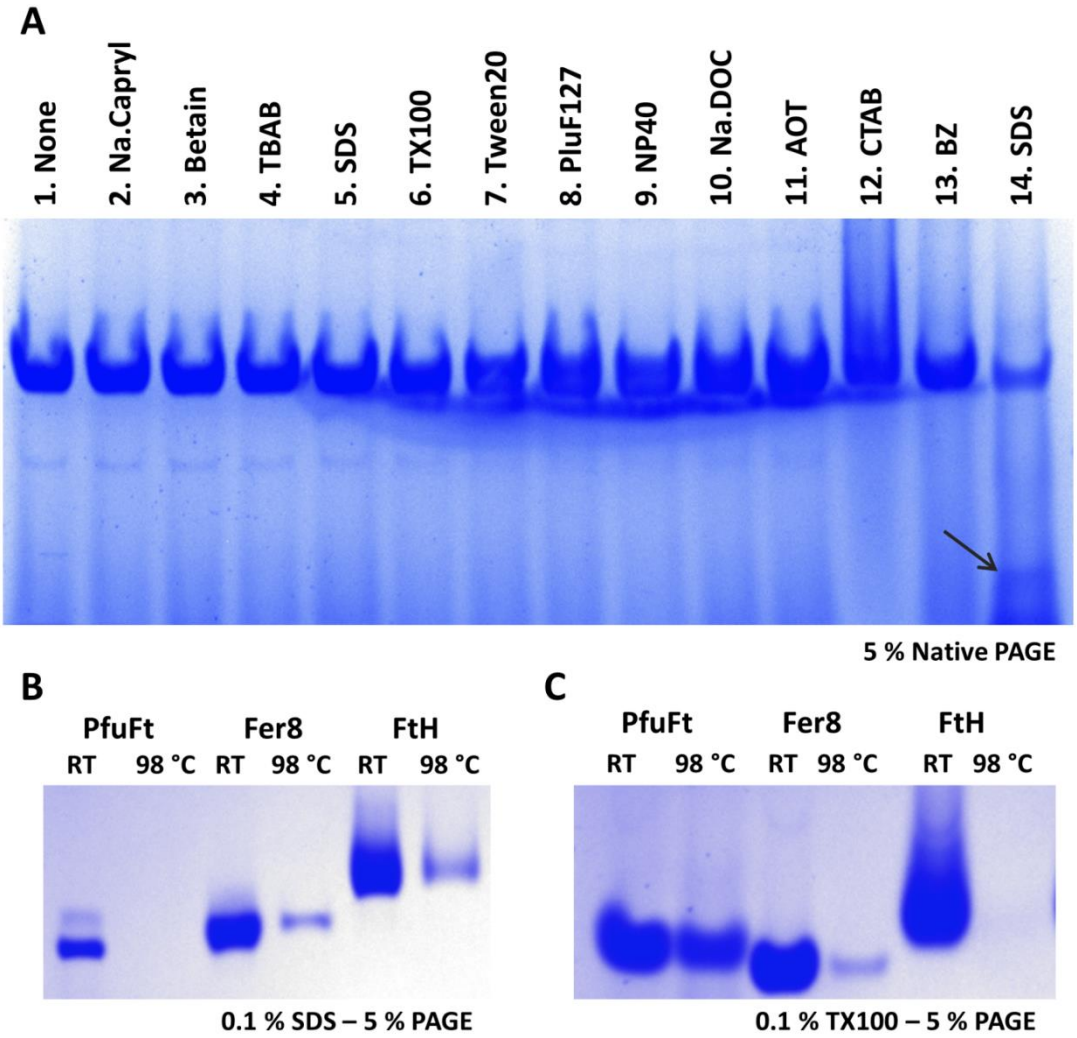


**Figure s2**. **PfuFt stability in detergents.** The stability of Pfu ferritin was determined by native PAGE (A). 20 μg of the protein sample was incubated in the presence of detergents at concentrations indicated in Table 1 for 2 hours at ambient temperature (conditions similar to those in presented chemical reactions) and separated on 5 % native PAGE. In all cases the protein migrates as 24mer similarly to sample without any detergent (line 1). Small amount of dimer can be detected only after 10 minutes of heating to 98 °C in presence of 1 mM SDS (line 14, arrow). In order to exclude the possibility of protein renaturation after the detergent dilution during electrophoresis we have analysed the protein migration in gels containing 0.1 % SDS (B) and 0.1 % Triton X100 (C) and compared Pfu stability with other ferritins, specifically horse L-chain ferritin (Fer8) and human H-chain ferritin (FtH). The proteins were incubated in presence of 1 % SDS or 1 % Triton X100 (concentrations exceeding those in reported catalytic reactions) for 1 hour or heated to 98 °C for 15 minutes and separated in gels containing the two selected detergents. All ferritins incubated at ambient temperature migrate

as closed 24mers in presence of SDS and Triton X100 indicating that the proteins remain intact in the reaction mix. Heating to 98 °C in presence of 1 % SDS leads to complete denaturation of Pfu and almost complete denaturation of Fer8 and FtH. Thermal treatment in presence of 1 %Triton X100 results in precipitation of mammalian ferritins while PfuFt remains intact. This further confirms extraordinary stability of Pfu ferritin.

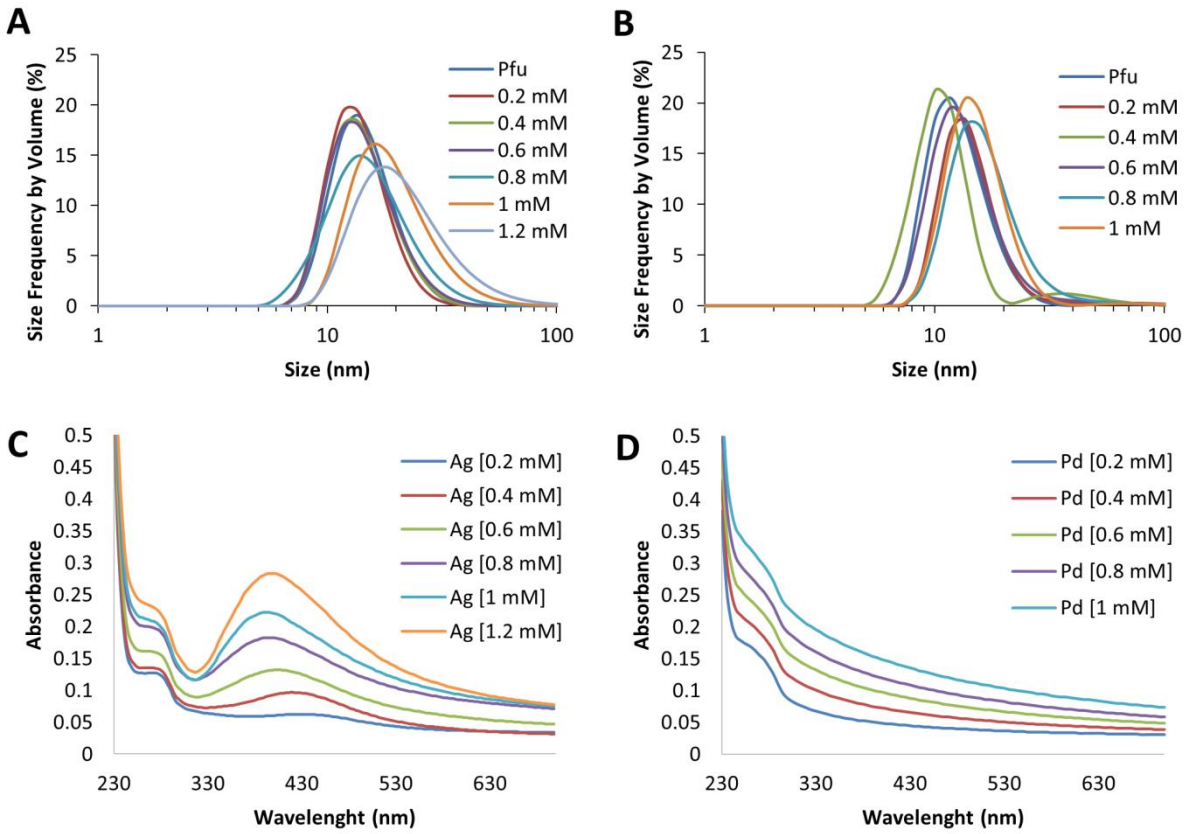


**Figure s3. Characterization of Ag/PfuFt and Pd/PfuFt by dynamic light scattering and UV-Vis absorption.** Dynamic light scattering (A, B) and UV-Vis absorption spectra (C, D) of Ag (A, C) and Pd (B, D) NPs synthesized in presence of PfuFt from different concentrations of the metal precursor. If the metal concentration exceeds 1 mM for $Ag^{+}$ and 0.8 mM for $Pd^{2+}$, the size of the complex measured by DLS increases, indicating the attachment of NPs to the surface of PfuFt. UV-Vis absorption spectra show absorption maximum at 400 nm typical for silver NPs. Pd NPs do not have any specific absorption peak.

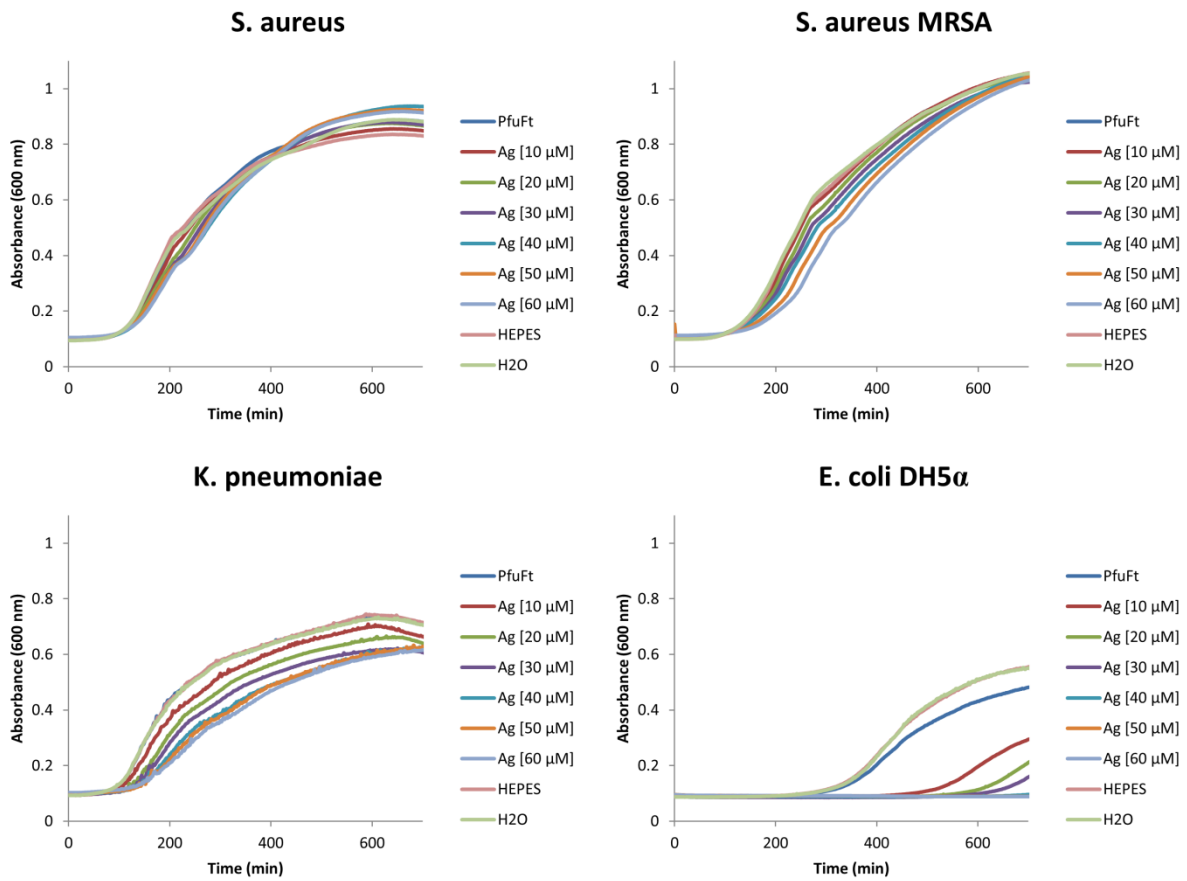


**Figure s4. Antibacterial activity of Ag/PfuFt.** The suppression of bacterial growth was analyzed in liquid culture for 12 h. The bacterial growth was measured as an increase in absorbance at 600 nm. Ag NPs in complex with PfuFt had no impact on the bacterial growth of *S. aureus* and *K. pneumoniae*. However, a strong inhibition of bacterial growth in culture of *E. coli* can be seen. Concentrations of silver (calculated as the concentration of $Ag^{+}$ precursor) in between 10 to 30 µM dramatically reduced bacterial growth and concentrations of 40 µM and higher entirely suppressed the growth of *E. coli*.

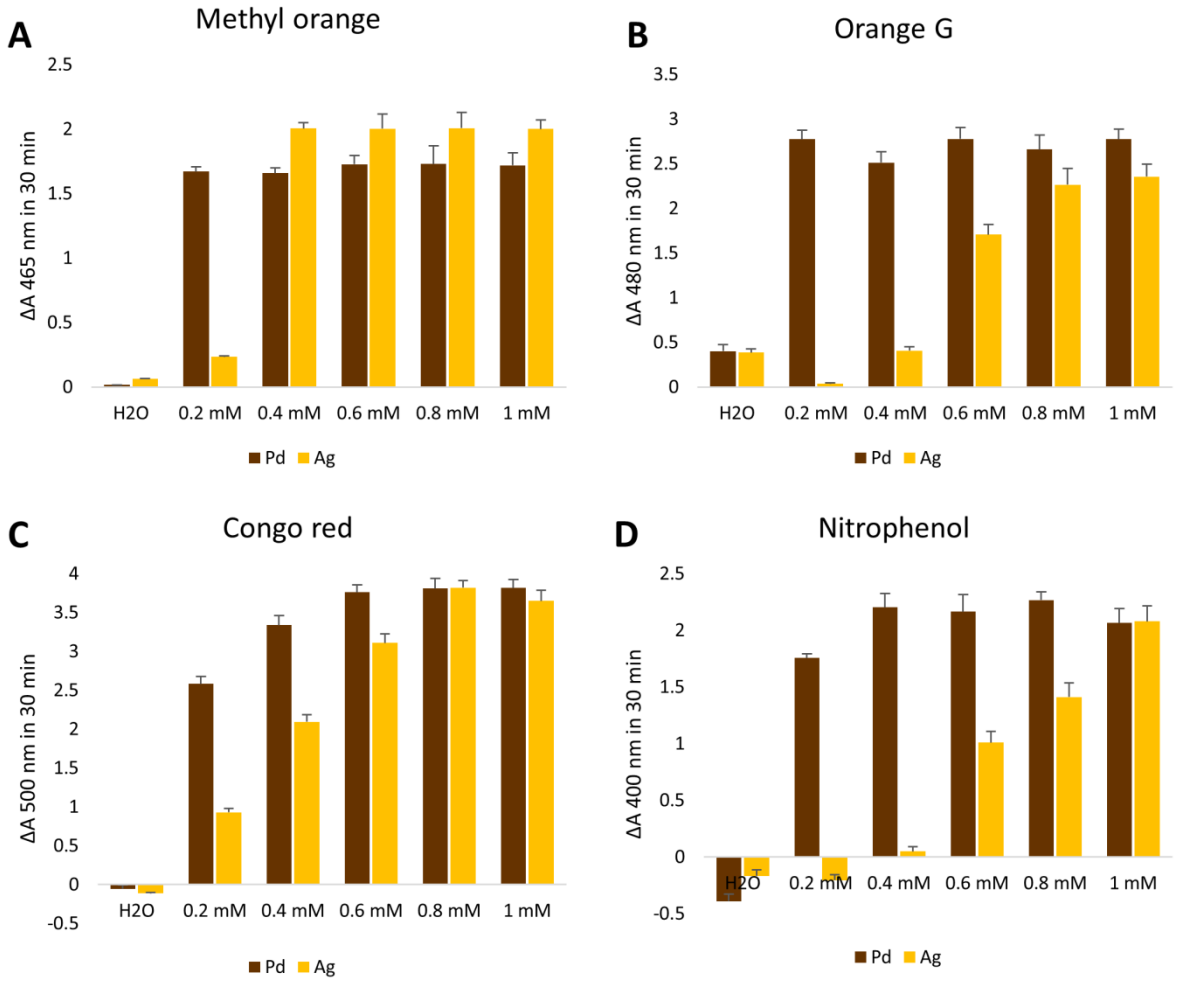


**Figure s5. Catalyzed decomposition of azo dyes and reduction of nitrophenol by metal NPs prepared from various amounts of metal precursor.** Methyl orange (A), Orange G (B), Congo red (C), and Nitrophenol (D) were reacted with $NaBH_4$ in presence of Ag and Pd NPs anchored to PfuFt for 30 min and the difference in absorbance (specified at each graph) was determined. The NPs were produced from different starting concentrations of the metal precursor as indicated at horizontal axis. Pd catalyzed reactions are in all cases more efficient compared to Ag catalyzed reactions.

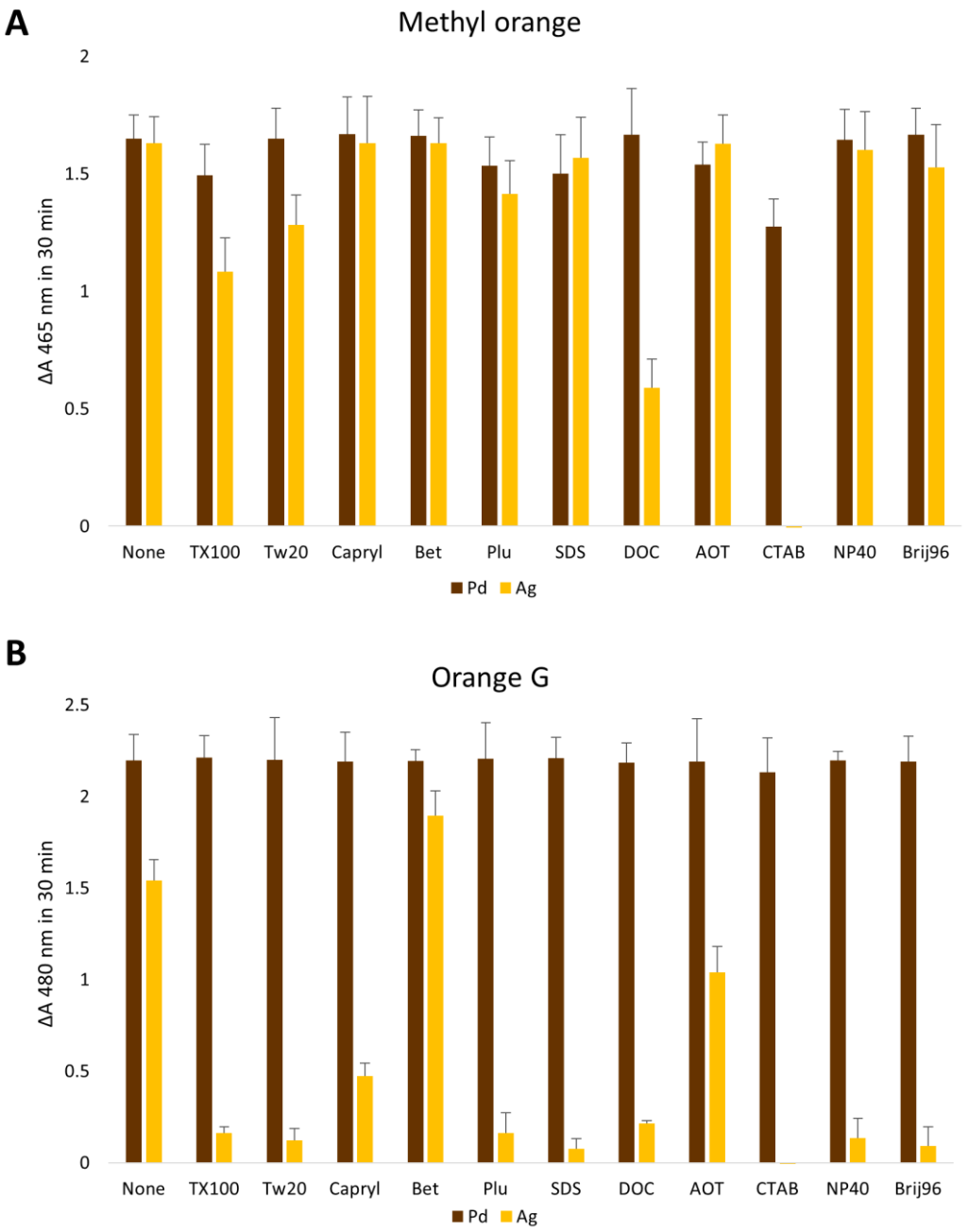


**Figure s6. Catalyzed decomposition of azo dyes by NPs in presence of detergents.** Substrates were reacted with $NaBH_4$ in presence of Ag and Pd NPs anchored to PfuFt for 30 min in presence of various detergents and the difference in absorbance (specified in each graph) was determined. The NPs were produced from 1 mM starting precursor concentrations and 0.5 μM ferritin concentration (PfuFt/Pd ratio = 1:2000).

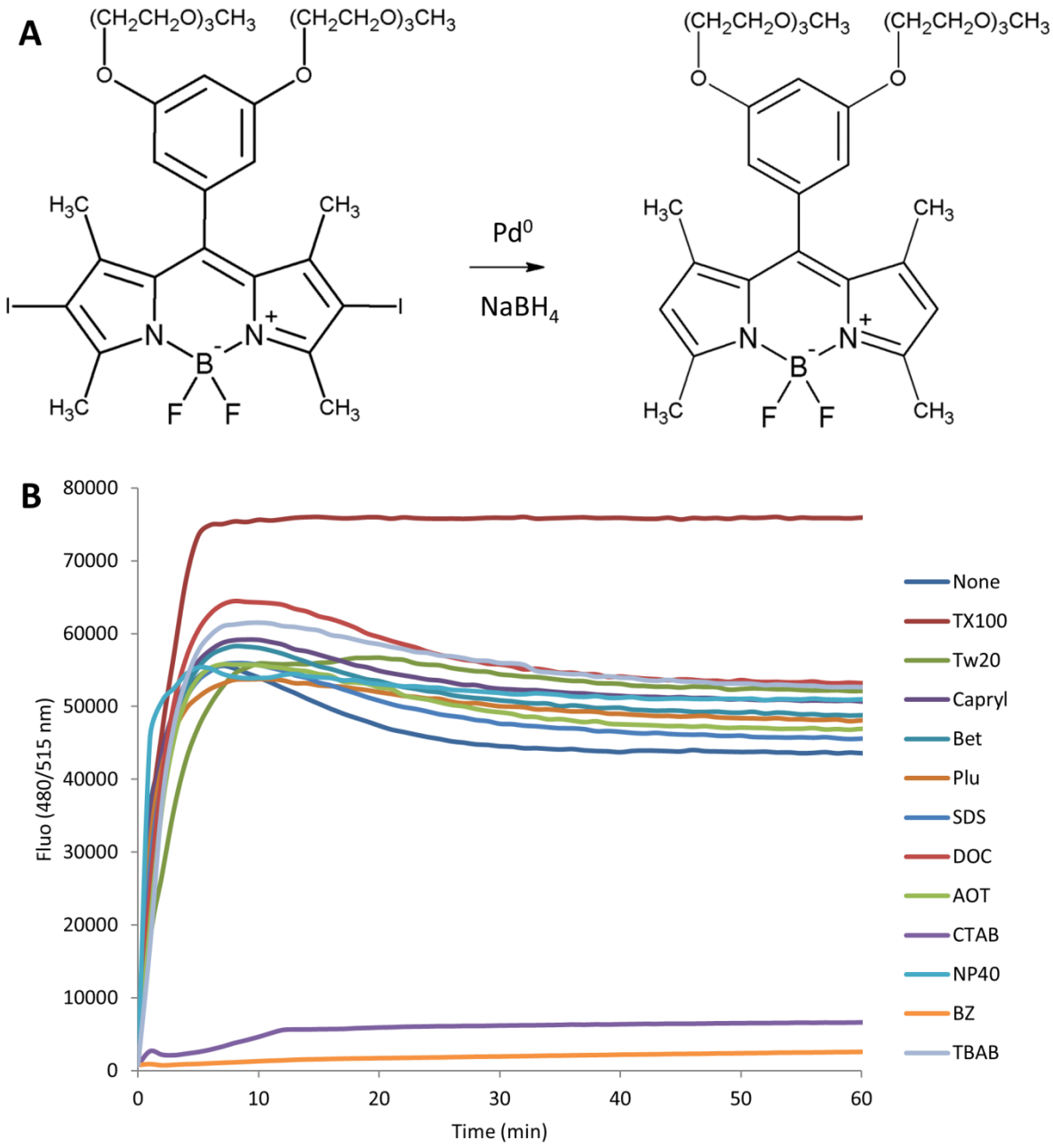


**Figure s7. Reductive dehalogenation of I.BODIPY**. Weakly red fluorescent I.BODIPY is catalytically converted into bright green fluorescent H.BODIPY (A). Reaction kinetics of the reaction is relatively fast as the reaction is completed within 5–10 min (B).

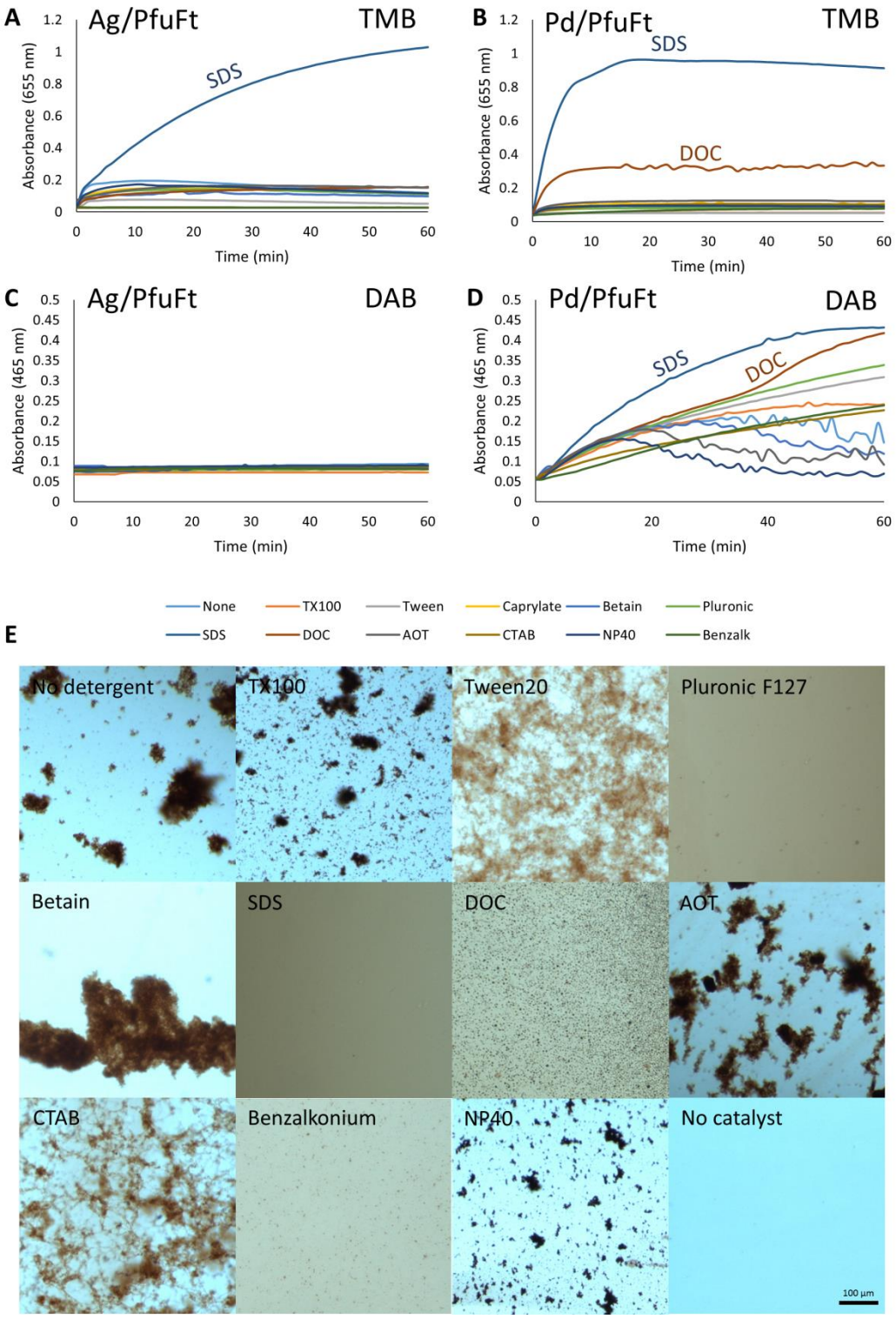


**Figure s8. Peroxidase activity of silver and palladium PfuFt NPs in presence of detergents.** The activity of Ag/PfuFt (A, C) and Pd/PfuFt (B, D, E) to convert tetramethylbenzidine (TMB, A, B) and diaminobenzidine (DAB, C, D, E) in presence of 2.5 mM hydrogen peroxide were measured. The structure of insoluble DAB precipitates in the presence of various detergents (E).

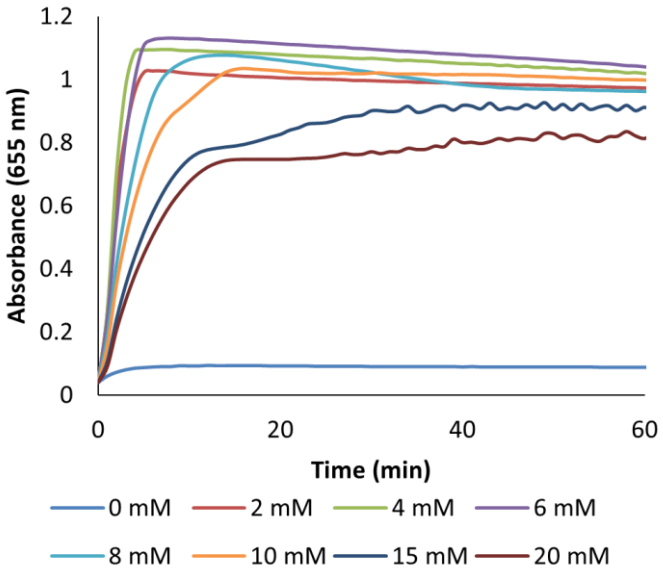


**Figure s9. Effect of different concentrations of SDS on peroxidase activity of Pd/PfuFt.** The formation of blue oxidation product of TMB has been followed by measurement of absorbance at 655 nm for 1 hour in 1 minute intervals at different concentrations of SDS. Concentrations of SDS exceeding 10 mM visibly inhibit the peroxidase activity.

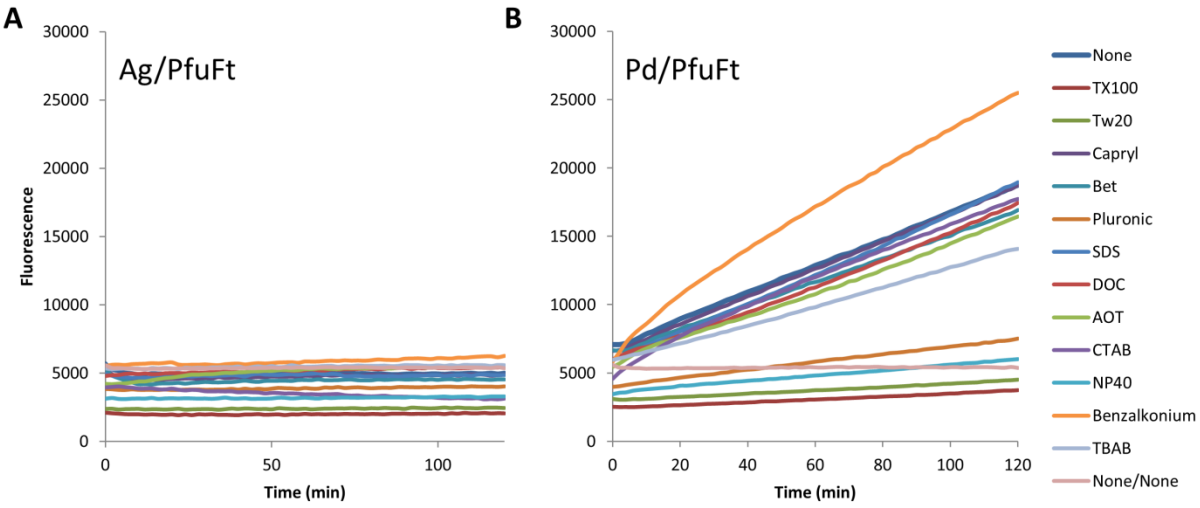


**Figure s10. Proc-R110 depropargylation.** Increase in fluorescence of Proc-R110 upon depropargylation in presence of Ag/PfuFt (A) and Pd/PfuFt (B) and various detergents.

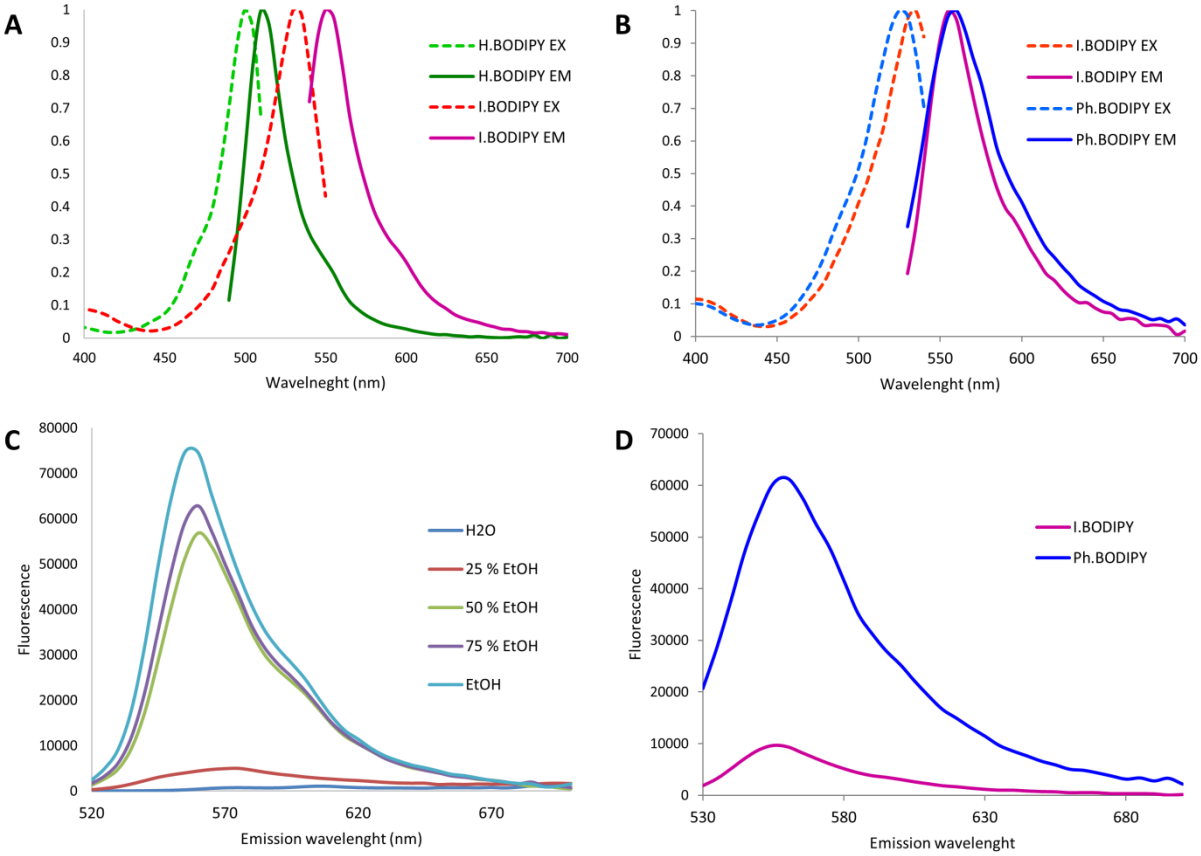


**Figure s11. Spectral characterization of I.BODIPY, H.BODIPY, and Ph.BODIPY.** Normalised spectra of H.BODIPY and I.BODIPY in EtOH (A), Ph.BODIPY and I.BODIPY in 50 % EtOH (B). Fluorescence of 100 µM I.BODIPY in different concentrations of EtOH (C) and relative fluorescence of 30 µM I.BODIPY and Ph.BODIPY in 50 % EtOH (D) measured at excitation 480 nm and gain 85.

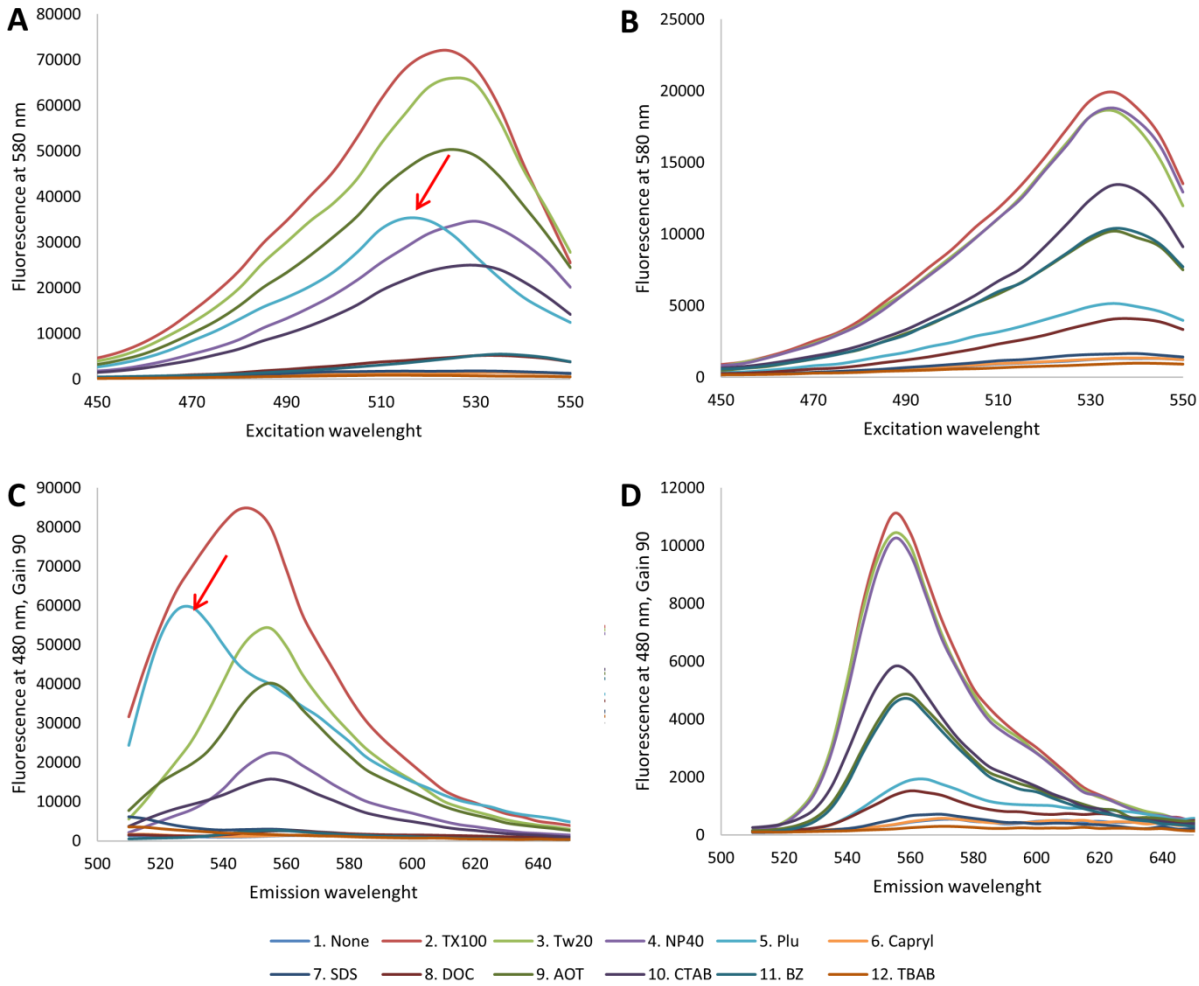


**Figure s12.** Excitation (A, B) and emission (C, D) scan of reaction products of Suzuki-Miyaura reaction between I.BODIPY and phenylboronic acid in presence of Pd/PfuFt catalyst (A, C) and in absence of a catalyst (B, D). Non-ionic detergents Triton X100, Tween 20 and NP40 increase fluorescence of I.BODIPY (D) to a greater extent than benzalkonium or CTAB. Presence of Pluronic F127 promotes I.BODIPY dehalogenation by Pd/PfuFt resulting in H.BODIPY with a distinct spectral shift in the excitation and emission spectra (arrow). Production of Phenyl.BODIPY increases the 525/560 nm fluorescence.
Note the different scale on the vertical axis.